# NJC

## Accepted Manuscript

This article can be cited before page numbers have been issued, to do this please use: N. Sekar, D. Patil, K. K. Sonigara, M. M. Jadhav, K. Avhad, S. Sharma and S. S. Soni, *New J. Chem.*, 2018, DOI: 10.1039/C7NJ04620K.


This is an Accepted Manuscript, which has been through the Royal Society of Chemistry peer review process and has been accepted for publication.

Accepted Manuscripts are published online shortly after acceptance, before technical editing, formatting and proof reading. Using this free service, authors can make their results available to the community, in citable form, before we publish the edited article. We will replace this Accepted Manuscript with the edited and formatted Advance Article as soon as it is available.

You can find more information about Accepted Manuscripts in the author guidelines.

Please note that technical editing may introduce minor changes to the text and/or graphics, which may alter content. The journal's standard Terms & Conditions and the ethical guidelines, outlined in our author and reviewer resource centre, still apply. In no event shall the Royal Society of Chemistry be held responsible for any errors or omissions in this Accepted Manuscript or any consequences arising from the use of any information it contains.

New Journal of Chemistry
View Article Online
DOI: 10.1039/C7NJ04620K

NJC

ARTICLE



# Effect of Structural Manipulation in Hetero-tri-aryl Amine Donor Based D-A'-π-A sensitizers in Dye Sensitized Solar Cells

Received 00th January 20xx,
Accepted 00th January 20xx

DOI: 10.1039/x0xx00000x

www.rsc.org/

Dinesh S. Patil,[a] Keval K. Sonigara,[b] Manoj M. Jadhav,[a] Kiran C. Avhad,[a] Suryapratap Sharma,[a] Saurabh S. Soni,[b,*] Nagaiyan Sekar[a,*]

The role of hetero-atom manipulation/hetero aryl group insertion in the triarylamine to have hetero triarylamine as a donor in highly efficient photosensitizers is focused to investigate the structure-efficiency relationship in the dye sensitized solar cell (DSSCs). Newly synthesized sensitizer contains N-phenyl-N-(pyridin-2-yl) pyridine-2-amine (DPPA) and N-(pyridin-2-yl)-N-(thiophen-2-yl) pyridine-2-amine (DPTA) as donor along with strong electron withdrawing cyano group (–CN) as auxiliary acceptor group while cyanoacetic acid and rhodamine-3-acetic acid are explored as anchoring groups. Triphenylamine donor is manipulated first time with the insertion of the nitrogen atom in aryl ring for DSSCs. These hetero aryls based sensitizer reflects significant improvement in photophysical as well as photovoltaic performance. The replacement of cyanoacetic acid by rhodanine-3-acetic acid as an anchoring unit results in a significant red shift in absorption and emission maxima. The methylene group in rhodanine-3-acetic acid interrupts the LUMO delocalization on anchoring group in sensitizers **DP3** and **DP4**, as shown by DFT calculations. The presence of cyanoacetic acid in sensitizers **DP1** and **DP2** shows effective charge transfer from HOMO to LUMO and efficient electron injection from LUMO to the conduction band of the $TiO_2$ semiconductor. The sensitizer **DP2** shows a maximum efficiency of 4.7%, short circuit current $J_{sc}$=11.78 mA.cm$^{-2}$, open circuit voltage $V_{oc}$=0.608 V and fill factor *FF*=0.62. The enhanced efficiency of sensitizer **DP2** has been attributed to the presence of strong electron withdrawing cyanoacetic acid anchoring group & presence of thiophene linker at N-aryl core.

## Introduction

Dye Sensitized Solar Cells (DSSCs) have gained significant importance in the past two decades due to the world demand for clean, renewable, environmental friendly and freely available energy sources [1]. Grätzel and co-workers in 1991 [2] reported the first dye sensitized solar cell based on ruthenium complex since then DSSCs research has gained revolutionary momentum [3–6]. Several metals based sensitizers have been synthesized in recent years and they have remarkable light to electricity conversion efficiencies [7–10]. However, tedious synthetic protocol, high metal cost, and environmental burden restricts their commercial exploration [11]. Therefore, metal free sensitizers are preferred in place of organometallic compounds [12]. The metal-free organic sensitizers have an advantage due to easy synthesis and purification process [13], economic desirability [14], high molar extinction coefficient [15] and ease in optimizing photophysical properties by structural modification. The efficient metal-free organic sensitizers have donor-π-acceptor (D-π-A) structure and modification of every part plays a significant role in altering the photovoltaic performance [16]. The photophysical, electrochemical and photovoltaic properties can be fined tuned by changing the donor part, π-linker or acceptor [17]. The different types of donating groups used in D-π-A type sensitizer includes coumarin [18], merocyanine [19], cyanine [20], indole [21], triphenylamine [22], thiophene [23], carbazole [24], phenothiazine [25], julolidine [26] and phenoxazine [27]. These donor units are attached with the acceptor units using various π-linkers which show moderate to high efficiencies [26–30]. Among these donors triphenyl amine based sensitizers have shown improved performance over the years [31]. The various strategies have been employed to boost the donating capacities of triphenyl amine by utilizing two donor ( D-D[32] 2D), two donor-pi system attached new donor {(D-π)2-D} [33], donor-pi-donor (D-π-D), auxiliary donor systems. The utilization pyridine based triphenyl amine based donor remains unexplored in DSSCs. In this paper we are reporting four novel molecules (DP1-DP4) based on N-phenyl-N-(pyridin-2-yl) pyridine-2-amine (DPPA) and N-(pyridin-2-yl)-N-(thiophen-2-yl) pyridine-2-amine (DPTA) as donor group for their potential application in DSSCs

[a] Department of Dyestuff Technology, Institute of Chemical Technology (ICT), Mumbai - 400 019, Maharashtra, INDIA
[b] Department of Chemistry, Sardar Patel University, Vallabh Vidyanagar - 388 120, Gujarat, INDIA
[c] * Authors to whom all correspondence will be done
[d] Email: sekar@gmail.com (Prof. N. Sekar)
[e] Email: soni_b21@yahoo.co.in (Prof. S. S. Soni)

Electronic Supplementary Information (ESI) available: [details of any supplementary information available should be included here]. See DOI: 10.1039/x0xx00000x

View Article Online
DOI: 10.1039/C7NJ04620K




(Scheme 1). We have used phenyl and thiophene as a pi- linker and cyano acetic acid and rhodanine-3-acetic acid as acceptor. Thiophene π-linker shows better performance over phenyl group as it has less delocalization of electron cloud over the ring and electron density is available for charge transfer which shows desirable polarizability, tuneable electrochemical and spectroscopic properties [34,35]. It plays significant role in electron conduction and affects the absorption and emission maxima of the sensitizers [36]. DP1 and DP2 were compared with their reported analogues to have established impact of donor manipulation on photophysical and photovoltaic properties [35].

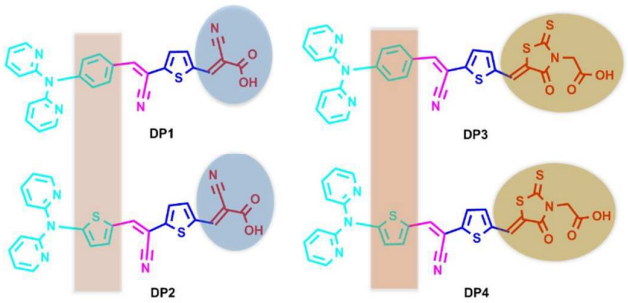


**Scheme 1.** Chemical structure of DP sensitizers

## Results and discussion

### Design and Synthesis of sensitizers

Scheme 2 and 3 explain the synthetic approach for the four sensitizers: DP1- DP4. The compound 1 was synthesized by the nucleophilic substitution reaction of 2-amino pyridine with 2-bromo pyridine. The nucleophilic substitution reaction between compound 1 and 4-bromo benzaldehyde and 5-bromo-thiophene-2-carboxaldehyde gives 2a and 2b respectively. The condensation of intermediates 2a and 2b with thiophene acetonitrile gives intermediates 3a and 3b, the Rieche formylation of 3a and 3b gives intermediates 4a and 4b. Knoevenagel condensation of intermediates 4a and 4b with cyanoacetic acid in the presence of piperidine resulted in the sensitizer DP1 (72% yield) and DP2 (76% yield) and with rhodamine-3-acetic acid in the presence of ammonium acetate resulted in the sensitizer DP3 (81% yield) and DP4 (84% yield) as final products.

### Photophysical properties

The UV-visible spectra of DP1-DP4 were recorded in N, N-dimethyl formamide ($2 \times 10^{-6}$ M) and the corresponding spectra are replicated in Fig. 1(a). The absorption maxima and molar extinction coefficient data in DMF for all sensitizers is given in Table 1. The sensitizers DP1 and DP2 show two absorption peaks in DMF. The first weak absorption peak lies in the range of 330-360 nm due to aromatic π-π* electron transition and second broad peak in the range of 370-600 nm broad peak is due to intramolecular charge transfer (ICT) [22] from DPPA and DPTA donor group to cyanoacetic acid acceptor group via thiophene π-bridge. DP3 and DP4 also show two absorption peaks in the range of 310-650 nm.

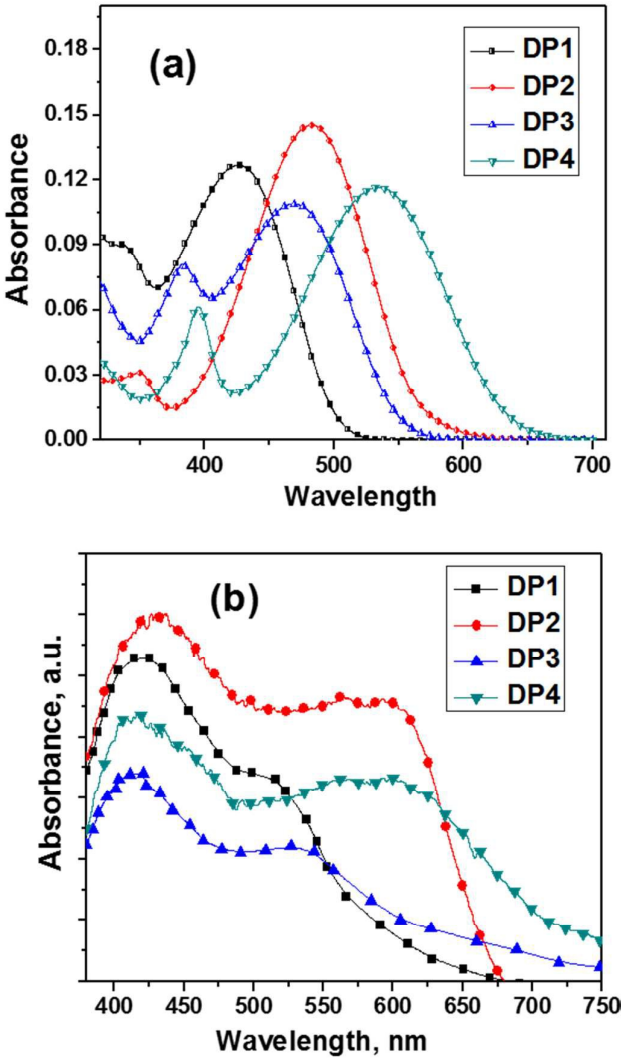


**Fig. 1.** (a) UV Visible of DP dyes recorded in DMF ($2 \times 10^{-6}$M), (b) UV-Visible reflectance spectra of dye coated $TiO_2$

The first absorption peak near 395 nm is very prominent which occurs due to aromatic π-π* electronic transition and second broad peak lies in the range of 430 to 650 nm is due to the intramolecular charge transfer (ICT) [37] from DPPA and DPTA (donor group) to rhodanine-3-acetic acid (acceptor group) via thiophene π-bridge. The sensitizers DP1 and DP3 are having same donor group and thiophene π-bridge but DP3 shows red shifted maxima. This red shift in maxima is due to rhodanine-3-acetic acid anchoring group manipulated as compared with DP1 having cyanoacetic acid. The red shift in DP3 in comparison with DP1 suggest that rhodanine-3-acetic acid is having better electron withdrawing capacity in comparison with cyano acetic acid which lowers the LUMO level of dye thus reducing the band gap. This is further proved by cyclic voltammetry data and DFT calculations. A similar trend has

View Article Online
DOI: 10.1039/C7NJ04620K




been observed between DP2 and DP4 having same donor group and thiophene π-bridge. DP4 have highest absorbance maxima value at 534 nm which is due to the presence of the thiophene π-bridge with the strong electron withdrawing cyano (CN) group which act as electron trap and rhodanine-3-acetic acid as an anchoring group. The sensitizer DP2 has comparatively high molar extinction coefficient value due to the presence of thiophene ring with CN group (act as electron trap) in π-bridge and universal famous anchoring group cyanoacetic acid which suggest good light harvesting capacity. The molar extinction coefficients values of DP1, DP2, DP3, and DP4 are 63,479, 72,512, 54,562 and 58,313 $M^{-1}$ $cm^{-1}$ respectively. Same trends were observed when we have measured UV-Visible reflectance spectra of dye loaded $TiO_2$ films (Fig. 1 (b)). Here, the observed broadening of spectra is compared with the spectra recorded in the solvent along with the red shift in the absorbance, confirms the anchoring of sensitizers on the nanocrystalline porous titania. DP3 and DP4 show red shift of 70 nm and 65 nm respectively and seems large broadening spectra indicates the poor charge transfer due to the rhodanine-3-acetic acid as anchoring group. Whereas, DP1 and DP2 show a lower broadening of spectra and large red shift of 82 nm and 81 nm for DP1 and DP2 respectively. This higher red shift indicates good charge transfer from donor to acceptor due to cyanoacrylic acid as strong acceptor as anchoring group and same is responsible for higher absorbance coefficient profile of DP1 and DP2 on $TiO_2$ surface.

### Electrochemical properties

The cyclic voltammetry (**Fig. 3a**) was used for the investigation of electrochemical properties of these four sensitizers to obtain the HOMO and LUMO energy level position of the sensitizers (**Table 1**). Under the application of the positive potential, CV showed two quasi-reversible oxidation waves which correspond to oxidation–reduction process. These two peaks were observed at 0.85 V and 1.25 V for **DP2** versus ferrocene/ferrocenium ($Fc/Fc^+$) was attributed to the oxidation of the $\pi$-conjugated backbone and donor, respectively.

Table 1

| Sensitizer | $\lambda_{max}$ [a] | $\lambda_{max}$ [b] | $\varepsilon_{max}$ [a] ($M^{-1}cm^{-1}$) | Onset vs. Ag/AgCl (V) | BG [c] (V) | HOMO [d] (eV) | LUMO [e] (V) |
|---|---|---|---|---|---|---|---|
| **DP1** | 426 | 508 | 63479 | 0.238 | 2.47 | 0.88 | -1.60 |
| **DP2** | 482 | 563 | 72512 | 0.507 | 2.17 | 1.13 | -1.03 |
| **DP3** | 468 | 538 | 54562 | 0.391 | 2.26 | 1.02 | -1.24 |
| **DP4** | 534 | 599 | 58313 | 0.437 | 1.95 | 1.07 | -0.88 |

*[a] Measured in DMF, [b] Measured from solid UV reflectance [c] Measured from $\lambda_{onset}$, [d] All potentials were obtained from CV. BG = Band gap, Potential measured vs. $Fc/Fc^+$ was converted to the NHE by the addition of +0.63 V. [d] Calculated from LUMO = HOMO – $E_g$.*

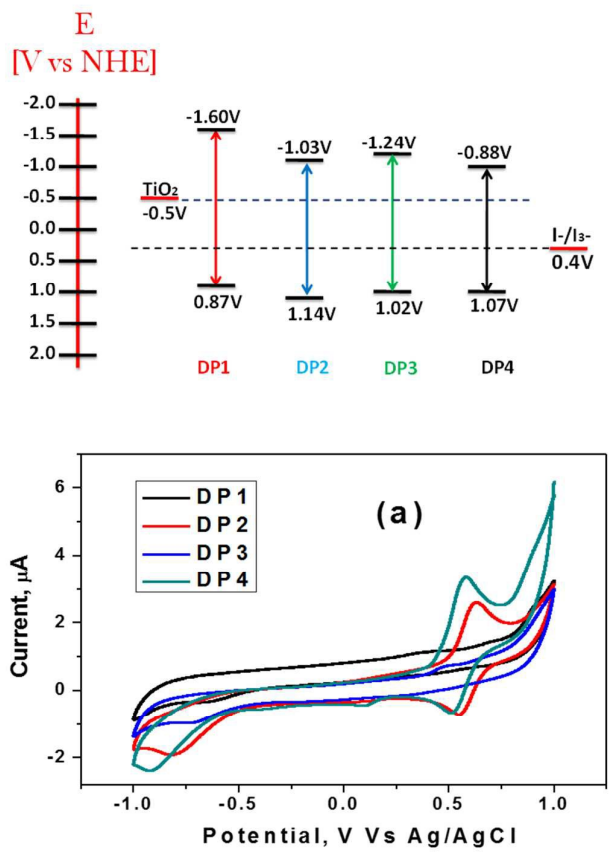


**Fig. 2.** (**a**) CV curves in acetonitrile at a scan rate of 25 mV/s, (**b**) Frontier molecular orbitals with the energy level diagram along with redox potentials of electrolyte (HOMOs; bottom) and (LUMOs; top) of the DP sensitizers.

The well-defined first oxidation peak for **DP2** compared to **DP1** confirms better charge transformation between D and A in the case of DPTA donor as compared to DPPA donor. The HOMO and LUMO energy levels of these four sensitizers were figured

View Article Online
DOI: 10.1039/C7NJ04620K




out from the DFT calculations and CV data which are summarized in **Table 1**.

The HOMO energy levels of **DP1**, **DP2**, **DP3,** and **DP4** are 0.87, 1.14, 1.02 and 1.07 V vs. the NHE (normal hydrogen electrode) respectively. These values are larger than the redox potential of $I^-/I_3^-$ redox couple (0.4 V vs. the NHE) of the electrolyte. This ensures a facile regeneration of the sensitizer by $I^-/I_3^-$ electrolyte after electron injection. The LUMO energy levels of **DP1**, **DP2**, **DP3**, and **DP4** are -1.60, -1.03, -1.24 and -0.88 V vs. NHE, respectively. The LUMO energy level of DP sensitizers is higher than the conduction band of $TiO_2$ (0.5 V vs. NHE), which indicates the feasibility of smooth electron injection on $TiO_2$ upon photo-excitation.

**Computational study**

Geometries of the sensitizers at their ground state were optimized by using the DFT global hybrid function B3LYP [38]. The basis set 6-31G (d) was used for all the atoms. The B3LYP is a combination of Becke's three parameter exchange functional

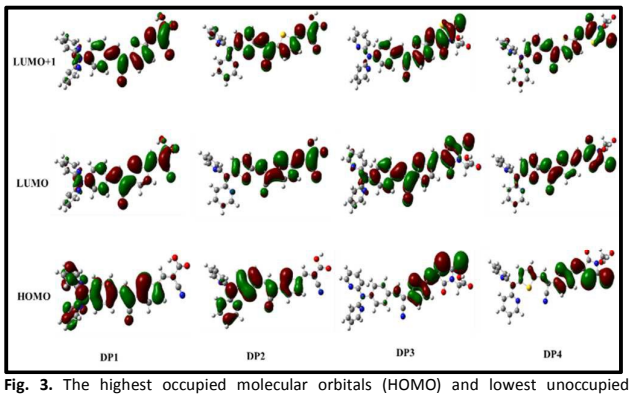


**Fig. 3.** The highest occupied molecular orbitals (HOMO) and lowest unoccupied molecular orbitals (LUMO) of all sensitizers. They were obtained at the B3LYP/6-31G(d) level in a vacuum.

(B3) [39] with the nonlocal correlation functional by Lee, Yang, and Parr (LYP) [40]. The first excited singlet states were optimized using TD-DFT B3LYP/6-31G(d) basis set. Frequency computations were also carried out on the optimized geometry of the low-lying vibronically relaxed first excited state of molecules [41]. The polarizable continuum model (PCM) [42,43] was used for optimization in a solvent (DMF). The Gaussian 09 program was used for DFT and TD-DFT computations [44]. Generally, the molecules which have both n – π* and π - π* states (D-π-A system), global hybrids such as B3LYP will generally provide an accurate estimate[45] and hence we preferred TD-DFT B3LYP method to perform the calculation.

The frontier molecular orbital diagram (FMO) of all the sensitizers are shown in **Fig. 2**, which shows that the electron density was uniformly distributed on the donor group in HOMO. On excitation electron cloud shifted towards the anchoring group at LUMO level, resulting in more effective intramolecular charge separation observed in sensitizers **DP1** and **DP2** as compared to the **DP3** and **DP4**. The charge delocalization from donor to acceptor on excitation encourages the effective injection of electrons into the conduction band of $TiO_2$ through the carboxyl anchoring group. The electronic distribution of HOMO and LUMO of all sensitizers at B3LYP/6-31G(d) level and their corresponding energy gap is shown in **Fig. S1** (**Table S1**). The HOMO-LUMO energy gap is high in the **DP1** as compared with the other sensitizers and in the case of **DP4,** it is low as compared with other sensitizers and the same results obtained from the cyclic voltammetry. The optimized geometries of all four sensitizers at B3LYP/6-31G(d) level shown in **Fig. S2** in SI.

The calculated electronic vertical transition energy, oscillator strengths (f), maximum absorption wavelength ($\lambda_{max}$) and nature of the transitions in various states are collected in **Table 2**. From Table 2, the strongest absorption peaks for all dyes mainly related to the transition from the HOMO to the LUMO. Moreover, one can find that the maximum absorption wavelength of **DP2** to **DP4** is remarkably red-shifted in DMF solution compared to **DP1** and **DP3** and the increased order is **DP1** < **DP3** < **DP2** < **DP4**. At the same time, the extent of the red-shift of **DP3** and **DP4** is larger, which can be explained by the difference of electronegativity for S atom and the better electron delocalization allowed by the sulphur atom in relation to the other atom. However, the red shift in sensitizer **DP2 and DP4** as compared with **DP1 and DP3** due to the thiophene (sulphur) ring present in **DP2 and DP4**. All sensitizers having D-A'-π-A configuration could be better as compared to the D-π-A structure. As a result, the calculated spectral data confirms that the introduction of the additional acceptor in D-A'-π-A system could be favourable for the long wavelength light-harvesting, and can be beneficial for enhanced photo-to-electric conversion efficiency of related solar cell as compared to D-π-A system [46].

The LHE is one of the significant parameter related to the intensity of the absorption spectra of the sensitizer and is calculated using the following equation (1), $LHE = 1–10^{-f}$

where f is the oscillator strength of the sensitizers. For an efficient photocurrent conversion, the value LHE of the sensitizers should be high. The LHE values were calculated for various bands of all sensitizers are shown in **Table S2**. The LHE of the sensitizers increases with an increase in red shift was observed in the **Table S2**. The maximum value of LHE around 0.984 by TD-B3LYP is observed for DP4. Generally, all sensitizers show LHE nearer to the unity, notably the DP2 show more power conversion efficiency compared to other sensitizers.

**Photovoltaic performance**

View Article Online
DOI: 10.1039/C7NJ04620K




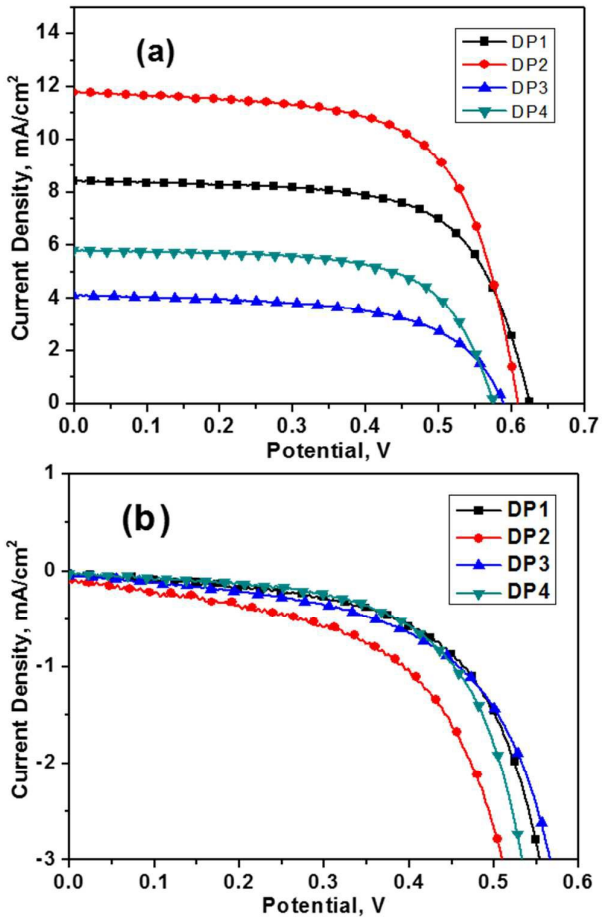


**Fig. 4.** *I–V* curves of the DSSCs, (a) with 1sun illumination and (b) without illumination in dark condition.

**Fig. 4a** shows the current–voltage characteristics of DSSCs fabricated with these dyes (**DP1** to **DP4**) as sensitizers under standard global AM 1.5 solar light conditions at 1 Sun illumination whereas **Fig. 4b** shows I-V characteristics in dark condition, which confirm the absence of dark reactions as all the devices give zero current density. The detailed parameters of short-circuit current density ($J_{sc}$), open-circuit voltage ($V_{oc}$), fill factor (*FF*), and photovoltaic conversion efficiency ($\eta$) are summarized in **Table 3.**

The short-circuit current $J_{sc}$ is correlated with a molar extinction coefficient of the sensitizers, hence the sensitizers with higher molar extinction coefficient yields the higher short-circuit current. The molar extinction coefficient of **DP2** is highest among all other **DP** series hence shows highest $J_{sc}$ = 11.78 mA/cm$^2$. The low $V_{oc}$ = 0.608 V of **DP2** in comparison with **DP1** is attributed due to low LUMO level with respect to **DP1**. The trend in photon light to current conversion efficiency was observed in the order **DP3** < **DP4** < **DP1** < **DP2. DP2** shows highest 4.7 % light to current conversion efficiency **(Table 3)**. **DP1** shows second highest photocurrent efficiency was 3.5 % and highest $V_{oc}$ was 0.624 V owing to the lowest $\lambda_{max}$ value, but it has beneficial properties like **DP2**. The lower performance of **DP3** and **DP4** is originated from the lower molar extinction coefficient and the week acceptor/anchoring group rhodanine-3-acetic acid, due to this the decrement in $J_{sc}$ value reflected in the device performance. Individually, between the **DP2** and **DP1**, keeping similar anchoring groups and the changing in donor portion from phenyl to thiophene group provides the hike in increasing molar absorption coefficient and $\lambda_{max}$ absorbance, which make **DP2** more efficient in photovoltaic performance. A similar trend was observed in the **DP3** and **DP4** moieties. Correlating **DP2** and **DP4**, the effect of different anchoring groups reveals the performance difference between the different capacity of charge injection into $TiO_2$ in $J_{sc}$ as well as $V_{oc}$ values. The **DP3** based DSSC showed $J_{sc}$ of 4.11 mAcm$^{-2}$, $V_{oc}$ of 0.589 V with a fill factor of 0.59. Visible difference in $V_{oc}$ parameters between **DP1/DP2** to **DP3/DP4** is related to negative shifting of $TiO_2$ conduction band after anchoring of sensitizer [47], the here strong cyanoacrylic acid group made a more negative shift of $TiO_2$ conduction band and results higher $V_{oc}$ compare to rhodanine-3-acetic acid.The photocurrent characteristics of the fabricated DSSCs are estimated from the incident photon-to-current conversion efficiency (*IPCE*) values measured at short-circuiting against the wavelength.

Table 2 Photovoltaic performance of DP based sensitizers.

| Sensitizers | $J_{sc}$(mA/cm$^2$) | $V_{oc}$ (V) | *FF* | $\eta$ (%) |
|---|---|---|---|---|
| **DP1** | 8.40 ± 0.20 | 0.624± 0.03 | 0.66 ± 0.05 | 3.5 ± 0.3 |
| **DP2** | 11.78 ± 0.20 | 0.608± 0.03 | 0.62 ± 0.05 | 4.7 ± 0.3 |
| **DP3** | 4.11 ± 0.20 | 0.589± 0.03 | 0.59 ± 0.05 | 1.5 ± 0.3 |
| **DP4** | 5.80 ± 0.20 | 0.575± 0.03 | 0.65 ± 0.05 | 2.2 ± 0.3 |

$J_{sc}$: short-circuit current, $V_{oc}$: open circuit voltage, ***ff:*** fill factor and ***PCE (%)***: *power* conversion efficiency.

All sensitizers show high fill factors (*FF*) between 59% and 66%. **Fig. S2** (SI) represents the IPCE spectra of the fabricated DSSCs exhibiting the highest values ~80–82% for **DP2** and other sensitizers showing a broad plateau in the wavelength range of 400–700 nm. The trend in IPCE spectra of the fabricated DSSCs was observed in the order **DP3** < **DP4** < **DP1** < **DP2.** This ensures a saturated light absorption by all the sensitizers DP1, DP2, DP3 and DP4, which is in good agreement with the UV–vis absorption spectra. It was important to note that the **DP2** show higher value of photon to current conversion efficiency, higher IPCE spectra value, higher molar extension coefficient, and higher $J_{sc}$ value.

### Electrochemical Impedance Spectroscopy and Tafel Characterization

To get more understanding of power conversion of DSSC devices based on different sensitizers, we have investigated the interfacial charge transfer process within DSSCs using the Electrochemical Impedance Spectroscopy (*EIS*) technique [48]. As shown in **Fig. 5** EIS showed two semicircles in the Nyquist plots for all sensitizers.

View Article Online
DOI: 10.1039/C7NJ04620K




The smaller (higher frequency from $10^3$ to $10^5$ Hz) and larger semi-circles (lower frequency from 1 to $10^2$ Hz) in the Nyquist plots are related to charge transfer at the counter electrode/electrolyte interface and the $TiO_2$/dye/electrolyte interface respectively. Third, the slightly visible arc is related to iodide diffusion in the electrolyte, it is very moderate due to use of liquid electrolyte [49]. First small arcs were almost similar in all the sensitizers which are due to the use of the same counter electrode and electrolyte components. In the EIS measurement, the curves were fitted using an equivalent circuit model (Inset of **Fig. 5**) and the obtained parameters are shown in **Table 4**. The recombination resistance of the **DP2** device was higher than that of the other devices according to the value derived from curve fitting in Z-view software. The trend observed for the recombination resistance are DP3 < DP4 < DP1 < DP2.

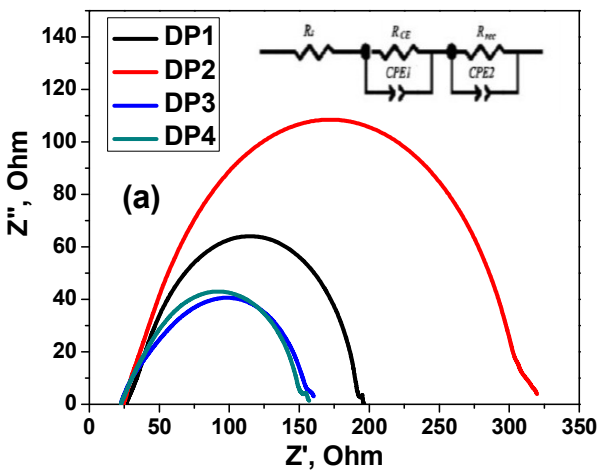


**Fig. 5.** EIS spectra of all devices in dark condition at -0.65 V DC forward bias. Inset of figure shows the equivalent circuit for fitting the Nyquist plot.

Table 3 DSSC parameters $R_{pt}$, $R_{rec}$, $t_n$ and $j_0$ extracted from *EIS* measurements and Tafel polarization study

| Name | $R_s$ [a] (Ω) | $R_{pt}$ [a] (Ω) | $R_{ct}$ [a] (Ω) | $C$ [a] (μF) | $\tau_r$ [a] (ms) | $\beta_a$ [b] (mV) | $\beta_c$ [b] (mV) | $j_0$ [b] (A/cm$^2$) |
|---|---|---|---|---|---|---|---|---|
| **DP1** | 26.82 | 13.19 | 164 | 7.22 | 1.86 | 108.5 | 212.1 | $3.01 \times 10^{-6}$ |
| **DP2** | 24.97 | 29.69 | 284 | 8.92 | 2.53 | 118.6 | 244.2 | $3.07 \times 10^{-6}$ |
| **DP3** | 23.04 | 16.05 | 140 | 3.05 | 0.27 | 98.36 | 203.0 | $1.12 \times 10^{-6}$ |
| **DP4** | 23.02 | 11.24 | 129 | 4.34 | 0.56 | 106.0 | 217.0 | $1.76 \times 10^{-6}$ |

[a] *Values estimated by fitting the Nyquist plot.* [b] *Estimated from Tafel polarization curves.*

DP3 and DP4 show lowest recombination resistance as compared to the other device. DP1 show the second highest value of recombination resistance. Electron lifetime ($\tau_r$) calculated for all the four devices is of the following order: **DP2** (2.53 ms) > **DP1** (1.86 ms) > **DP4** (0.56 ms) > **DP3** (0.27 ms). Here, the higher electron lifetime $\tau_r$ indicates the lower recombination of an electron from $TiO_2$ to the electrolyte and it results in the higher $J_{sc}$ value [50]. Based on said phenomenon the trend is in good agreement with the variation tendency of $J_{sc}$ observed in the *J–V* curves.

To support the phenomena observed from the EIS characteristics, Tafel polarization technique [51] is used to study better understanding of the recombination kinetics of electrolyte and electrode component of the solar cells (**Fig. 6**). Tafel analysis tells in brief on the interfacial charge transfer of electrolyte redox couple at the catalyst platinum electrode and oxidation/reduction reaction exhibit at the semiconductor electrolyte interface which can be understood by the help of Buttler-Volmer equation [52]. The nature of Tafel plots looks very similar and it indicates the similar smooth catalytic reaction at the counter electrode and electrolyte interface. Tafel measurement data was fitted using corrview software and the exchange current density was estimated for all devices.

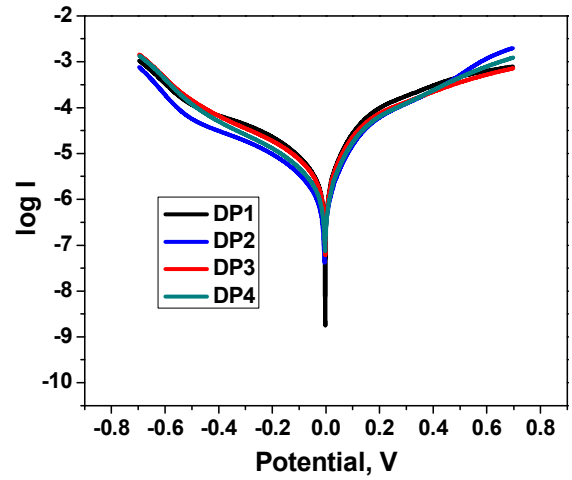


**Fig. 6** Tafel polarization curve of DSSCs taken in dark.

Order of exchange current density well supports the recombination resistance extracted from the EIS spectra and while the well proved obtained *I-V* performance of the DSSC performed with these dyes.

## Experimental

### Materials and Methods

All chemicals and synthetic reagents required for synthesis are procured from S. D. Fine Chemicals. 3-methoxy propionitrile (MNP), Guanidinium thiocyanate (GSCN), 4-*tert* butyl pyridine (TBP), Iodine, 1-butyl-3-methylimidazolium iodide were purchased from Sigma-Aldrich and TCI chemicals. FTO substrates (7Ω/cm$^2$) and hot melt tape were purchased from Solaronix Inc, Switzerland. 0.25 mm silica gel 60 F254 percolated plates on alumina is used for monitoring the reaction progress, which was visualized with UV light. $^1$H-NMR and $^{13}$C-NMR spectra were recorded on Agilent technology 500-MHz instrument by using TMS as an internal standard. The

View Article Online
DOI: 10.1039/C7NJ04620K




UV-visible absorption spectra of the compounds were recorded on a Perkin-Elmer Lambda- 25 spectrometers. The solid UV-visible reflectance of dye loaded $TiO_2$ performed using Ocean optics spectrometer analyzing with spectra suite software. Cyclic Voltammetry (CV) was performed with (CH instruments model 660E) electrochemical workstation with three standard electrochemical cells. Dye solution prepared in acetonitrile and platinum disc was used as a working electrode, $Ag/Ag^+$ electrode as the reference and Pt wire as counter electrode. 0.1 M tetrabutylammonium hexafluorophosphate ($TBAPF_6$) dissolved in acetonitrile solvent is used as supporting electrolyte. CV curves were calibrated by using ferrocene as the standard. The photocurrent density-voltage (*J-V*) characteristics of the fabricated DSSCs were measured by using Keithly-2450 digital source meter controlled by a computer scan rate of 10 $mVs^{-1}$. A solar simulator (PET 80AAA, USA) 300 W xenon lamp, connected with an AM 1.5 G filter to serve as the light source, give $100mW/cm^2$ at the surface of the test cell to remove ultraviolet and infrared radiation. While Electrochemical and Impedance measurements were carried out using SOLARTRON electrochemical analyzer (Solartron 1287 + 1260). The impedance of the DSSC was measured by sweeping low amplitude AC signal (10 mV) having a frequency ranging from 120 kHz to 0.1 Hz. During the measurement, cells were held in dark under the application of -0.70 V DC bias. Tafel polarization curves were obtained by sweeping potential from -0.7 to 0.7 to the DSSC in dark and resulting data were fitted in Buttler-Volmer equation.

**Synthesis**

**Di(pyridin-2-yl) amine (1)**

2-Amino pyridine (5.31 mmol) and 2-bromo pyridine (6.37 mmol) in toluene (50ml) were added to a round bottom flask equipped with a condenser. NaH (5.31 mmol) added slowly to the reaction mixture. In addition, the reaction mixture was heated under reflux condition for 24 h. The reaction was monitored using TLC (eluent: 40% ethyl acetate in hexane). After completion of the reaction, the reaction mass was poured into water. The organic layer was separated and washed, several times with water and then dried over anhydrous sodium sulfate. The dried organic layer was evaporated on a rotary evaporator. The resulting residue was purified by column chromatography using ethyl acetate/hexane (40:60), thereby affording the desired product as a white solid 1 (Yield: 51%).

$^1$H NMR (500 MHz, $CDCl_3$) $\delta_{ppm}$ 8.28 (ddd, *J* = 5.0, 1.8, 0.8 Hz, 2H), 8.01 (s, 1H), 7.62 – 7.55 (m, 4H), 6.86 – 6.83 (m, 2H).

$^{13}$C NMR (125 MHz, $CDCl_3$) $\delta_{ppm}$ 154.10, 147.74, 137.72, 116.33, 111.67.

**4-(Di(pyridin-2-yl) amino) benzaldehyde (2a)**

The compound 1 (0.7 mmol) and p-bromo benzaldehyde (0.84 mmol) was dissolved in DMF (12 ml) then subsequent added $K_2CO_3$ (0.84 mmol) and Cu(I) (0.14 mmol) in a 20ml microwave vial, and irradiation of microwave for 55 minutes with 10 bar pressures and 200 $^0$C temperature. After completion of the reaction (monitored by TLC), the reaction mixture was cooled to room temperature and poured into ice water. The crude product was extracted with ethyl acetate and the organic layer was washed with water and dried over anhydrous sodium sulphate. After removing the solvent under reduced pressure, the residue was purified by column chromatography using ethyl acetate/hexane (40:60) to afford the light yellow solid 2a (48% yield).

$^1$H NMR (500 MHz, $CDCl_3$) $\delta_{ppm}$ 9.92 (s, 1H), 8.39 (dd, *J* = 5.1, 2.0 Hz, 2H), 7.83 (d, *J* = 8.5 Hz, 2H), 7.65 (td, *J* = 7.8, 2.0 Hz, 2H), 7.23 (d, *J* = 8.6 Hz, 2H), 7.07 – 7.04 (m, 4H).

$^{13}$C NMR (125 MHz, $CDCl_3$) $\delta_{ppm}$ 190.92, 157.50, 150.70, 149.11, 138.13, 131.13, 124.70, 119.70, 118.37.

**5-(Di(pyridin-2-yl) amino) thiophene-2-carbaldehyde (2b)**

In 50ml sealed tube 5-bromo thiophene-2-carboxaldehyde (0.84 mmol) and compound 1 (0.7 mmol) were dissolved in DMF (15ml), then added $K_2CO_3$ (0.84 mmol) and Cu(I)I (0.14 mmol) in the reaction mixture. The sealed tube was kept for heating at 150$^0$C for 16 hours. After completion of the reaction (monitored by TLC), the reaction mixture was cooled to room temperature and poured into ice water. The crude product was extracted with ethyl acetate and the organic layer washed with water and dried over anhydrous sodium sulphate. After removing the solvent under reduced pressure, the residue was purified by column chromatography using eluent ethyl acetate/hexane (40:60) to afford the light yellow solid 2b (43% yield).

$^1$H NMR (500 MHz, DMSO) $\delta_{ppm}$ 9.73 (s, 1H), 8.60 (dd, *J* = 4.9, 1.7 Hz, 2H), 7.91 (td, *J* = 7.8, 1.9 Hz, 2H), 7.68 (d, *J* = 4.4 Hz, 1H), 7.36 (dd, *J* = 7.3, 4.9 Hz, 2H), 6.97 (d, *J* = 8.2 Hz, 2H), 6.02 (d, *J* = 4.4 Hz, 1H).

$^{13}$C NMR (125 MHz, DMSO) $\delta_{ppm}$ 184.06, 154.83, 153.92, 149.20, 140.12, 137.31, 133.44, 121.67, 118.08, 114.02.

**(E)-3-(4-(Di(pyridin-2-yl) amino) phenyl)-2-(thiophen-2-yl) acrylonitrile (3a)**

In 50ml round bottom flask, 2 to 3 drops of piperidine were added to a solution of the compound 2a (0.29 mmol) and thiophene acetonitrile (0.34 mmol) in ethanol (12 ml). The reaction mixture was refluxed for 6 h. After completion of the reaction (monitored by TLC), the reaction mixture was cooled to room temperature and poured into ice water. The crude product was extracted with ethyl acetate and the organic layer washed with water and dried over anhydrous sodium sulphate. After removing the solvent under reduced pressure, the residue purified by column chromatography using eluent ethyl acetate/hexane (40:60) to afford the yellow solid 3a (84% yield).

$^1$H NMR (500 MHz, $CDCl_3$) $\delta_{ppm}$ 8.37 (d, *J* = 4.7 Hz, 1H), 8.35 (d, *J* = 4.8 Hz, 1H), 7.84 (d, *J* = 8.6 Hz, 1H), 7.63 (d, *J* = 8.1 Hz, 1H), 7.59 (d, *J* = 9.9 Hz, 1H), 7.39 – 7.31 (m, 2H), 7.29 (d, *J* = 6.7 Hz, 2H), 7.23 (d, *J* = 8.4 Hz, 1H), 7.20 (d, *J* = 8.6 Hz, 1H), 7.05 (d, *J* = 7.6 Hz, 2H), 7.03 – 6.97 (m, 3H).

View Article Online
DOI: 10.1039/C7NJ04620K




**(E)-3-(5-(Di(pyridin-2-yl) amino) thiophen-2-yl)-2-(thiophen-2-yl) acrylonitrile (3b)**

This was prepared as described in the preparation of 3a. The residue of the 3b was purified by column chromatography using eluent ethyl acetate/hexane (40:60) to afford orange solid 3b (81% yield).

$^{1}$H NMR (500 MHz, $CDCl_3$) δ 8.47 (dd, *J* = 4.9, 1.3 Hz, 2H), 7.69 – 7.65 (m, 2H), 7.40 (d, *J* = 4.2 Hz, 1H), 7.36 (s, 1H), 7.26 (d, *J* = 3.5 Hz, 1H), 7.23 (dd, *J* = 5.1, 0.9 Hz, 1H), 7.09 (dd, *J* = 7.2, 5.0 Hz, 2H), 7.04 – 6.99 (m, 3H), 6.48 (d, *J* = 4.2 Hz, 1H).

$^{13}$C NMR (126 MHz, $CDCl_3$) δ 155.91, 151.55, 148.75, 139.34, 138.33, 132.90, 131.43, 131.37, 128.10, 125.99, 125.19, 119.89, 119.32, 117.53, 117.05, 100.18.

**(E)-3-(4-(Di(pyridin-2-yl) amino) phenyl)-2-(5-formylthiophen-2-yl) acrylonitrile (4a)**

The dichloromethyl methyl ether (0.52 mmol) was added to a solution of the compound 3a (0.17 mmol) in dichloromethane (12 ml) at 0°C. $TiCl_4$ (0.52 mmol) was then added dropwise to the above solution. The reaction mixture was stirred at room temperature for 0.5 h. After completion of the reaction (monitored by TLC), the reaction mixture was poured into cold dilute HCl solution. The crude product was extracted into dichloromethane and the organic layer was washed with water and dried over anhydrous sodium sulphate. After removing the solvent under reduced pressure, the residue was purified by column chromatography using eluent ethyl acetate/hexane (40:60) to afford the orange solid 4a (83% yield).

$^{1}$H NMR (500 MHz, $CDCl_3$) $\delta_{ppm}$ 9.89 (s, 1H), 8.39 (dd, *J* = 4.9, 1.9 Hz, 2H), 7.89 (d, *J* = 8.7 Hz, 2H), 7.72 (d, *J* = 4.0 Hz, 1H), 7.66 – 7.63 (m, 2H), 7.50 (s, 1H), 7.44 (d, *J* = 3.9 Hz, 1H), 7.22 – 7.20 (m, 2H), 7.08 – 7.04 (m, 4H).

$^{13}$C NMR (126 MHz, $CDCl_3$) $\delta_{ppm}$ 182.46, 157.45, 149.09, 148.95, 148.57, 148.19, 142.72, 142.36, 138.05, 136.87, 131.16, 130.88, 128.28, 127.13, 125.14, 119.56, 118.22, 116.37, 103.19.

**(E)-3-(5-(Di(pyridin-2-yl) amino) thiophen-2-yl)-2-(5-formylthiophen-2-yl) acrylonitrile (4b)**

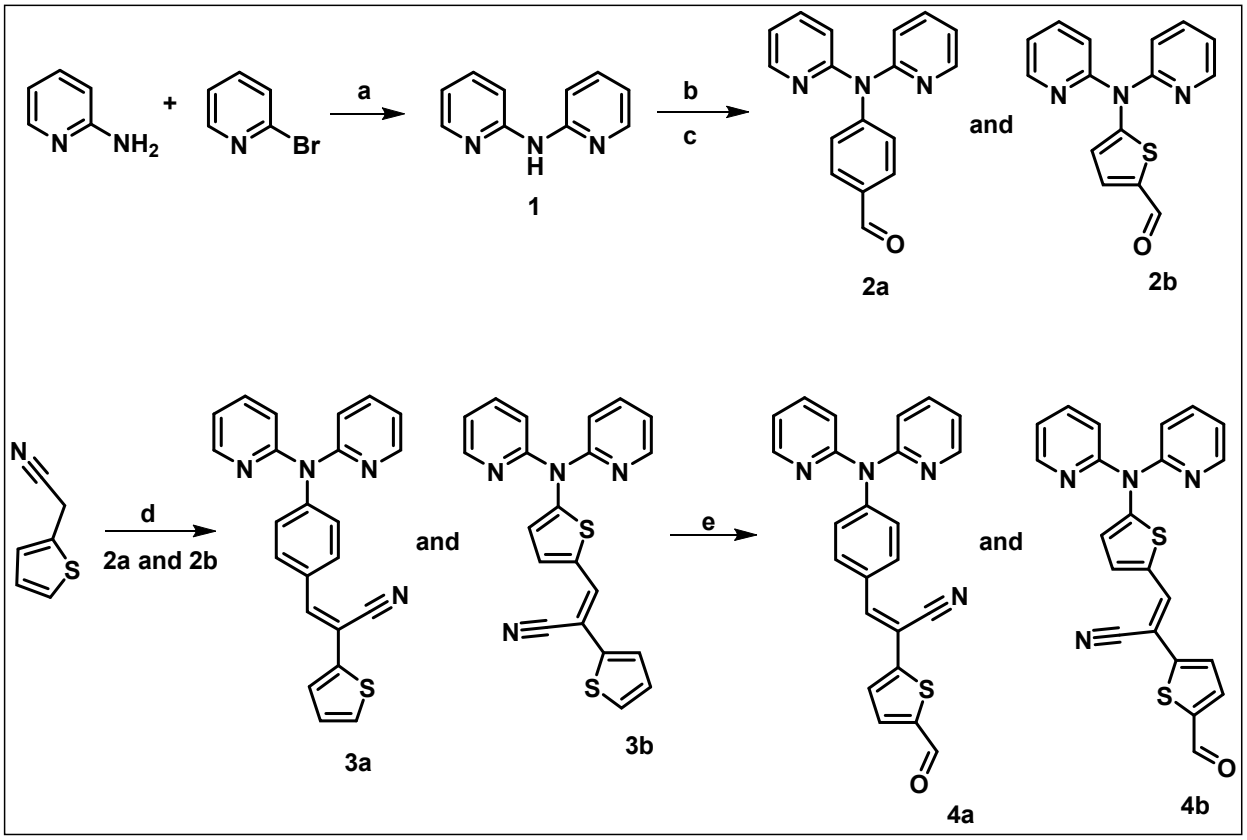


**Scheme 2.** Synthesis of intermediat: (a) NaH, toluene, reflux (b) 4-bromo-benzaldehyde, $K_2CO_3$, Cu(I), microwave. (c) 5-bromo-thiophene-2-carboxaldehyde, $K_2CO_3$, Cu(I), seal tube. (d) thiophene acetonitrile, piperidine, ethanol, reflux. (e) $TiCl_4$, dichloromethyl methyl ether, DCM, R.T.

This was prepared as described in the preparation of 4a. The residue of the 4b was purified by column chromatography using eluent ethyl acetate/hexane (40:60) to afford red solid 4b (78% yield).

$^{1}$H NMR (500 MHz, $CDCl_3$) $\delta_{ppm}$ 9.83 (s, 1H), 8.55 (dd, *J* = 4.9, 1.3 Hz, 2H), 7.74 – 7.70 (m, 2H), 7.67 (d, *J* = 4.0 Hz, 1H), 7.54 (s, 1H), 7.49 (d, *J* = 4.4 Hz, 1H), 7.30 (d, *J* = 4.0 Hz, 1H), 7.18 (ddd, *J*

View Article Online
DOI: 10.1039/C7NJ04620K


= 7.3, 4.9, 0.6 Hz, 2H), 6.95 (d, *J* = 8.2 Hz, 2H), 6.29 (d, *J* = 4.4 Hz, 1H).
$^{13}$C NMR (126 MHz, $CDCl_3$) $\delta_{ppm}$ 182.27, 154.82, 153.59, 149.40, 148.90, 141.61, 138.71, 137.30, 136.33, 133.55, 129.34, 125.78, 120.57, 117.38, 117.10, 116.67, 97.47.

**(E)-2-Cyano-3-(5-((E)-1-cyano-2-(4-(di(pyridin-2-yl) amino) phenyl) vinyl) thiophen-2-yl) acrylic acid (DP1)**

Two to three drops of piperidine were added to a solution of the compound 4a (0.0526 mmol) and cyanoacetic acid (0.105 mmol) in acetonitrile (5 ml). The reaction mixture was refluxed for 3.5 hrs. After completion of the reaction (monitored by TLC), the reaction mixture was cooled to room temperature and poured into water. The product filtered washed with water then purified by solvent treatment (wash with diethyl ether) to afford compound **DP1** as a red solid (72% yield).
$^{1}$H NMR (500 MHz, DMSO) $\delta_{ppm}$ 8.49 (s, 1H), 8.31 (dd, *J* = 4.8, 1.3 Hz, 2H), 8.00 (d, *J* = 4.0 Hz, 2H), 7.96 (d, *J* = 8.8 Hz, 2H), 7.77 – 7.74 (m, 2H), 7.64 (d, *J* = 4.0 Hz, 1H), 7.17 – 7.12 (m, 4H), 7.04 (d, *J* = 8.3 Hz, 2H).
$^{13}$C NMR (125 MHz, DMSO) $\delta_{ppm}$ 163.73, 157.46, 149.05, 148.37, 147.63, 146.33, 143.60, 141.00, 138.86, 136.00, 131.40, 128.70, 127.16, 125.42, 120.11, 118.50, 117.23, 116.80, 102.23, 100.52.
Elemental Analysis- Calculated: C, 68.20; H, 3.60; N, 14.73; O, 6.73; S, 6.74.
Found: C, 68.23; H, 3.59; N, 14.75.

**(E)-2-Cyano-3-(5-((E)-1-cyano-2-(5-(di(pyridin-2-yl) amino) thiophen-2-yl) vinyl) thiophen-2-yl) acrylic acid (DP2)**

This was prepared as described in the preparation of **DP1**. The residue was purified by solvent treatment (wash with diethyl ether) to afford compound **DP2** as dark red solid (76% yield).
$^{1}$H NMR (500 MHz, DMSO) $\delta_{ppm}$ 8.52 (d, *J* = 3.8 Hz, 2H), 7.99 (d, *J* = 8.1 Hz, 2H), 7.91 – 7.86 (m, 2H), 7.63 (dd, *J* = 19.5, 4.1 Hz, 2H), 7.35 (d, *J* = 3.9 Hz, 1H), 7.31 (dd, *J* = 6.9, 5.2 Hz, 2H), 7.01 (d, *J* = 8.2 Hz, 2H), 6.23 (d, *J* = 4.2 Hz, 1H).
$^{13}$C NMR (125 MHz, DMSO) $\delta_{ppm}$ 162.76, 154.58, 152.57, 149.10, 143.98, 139.86, 136.95, 136.53, 136.41, 135.18, 129.35, 125.42, 121.35, 119.70, 118.00, 117.89, 116.40, 96.35.
Elemental Analysis- Calculated: C, 62.36; H, 3.14; N, 14.54; O, 6.64; S, 13.32.
Found: C, 62.39; H, 3.13; N, 14.56.

View Article Online
DOI: 10.1039/C7NJ04620K




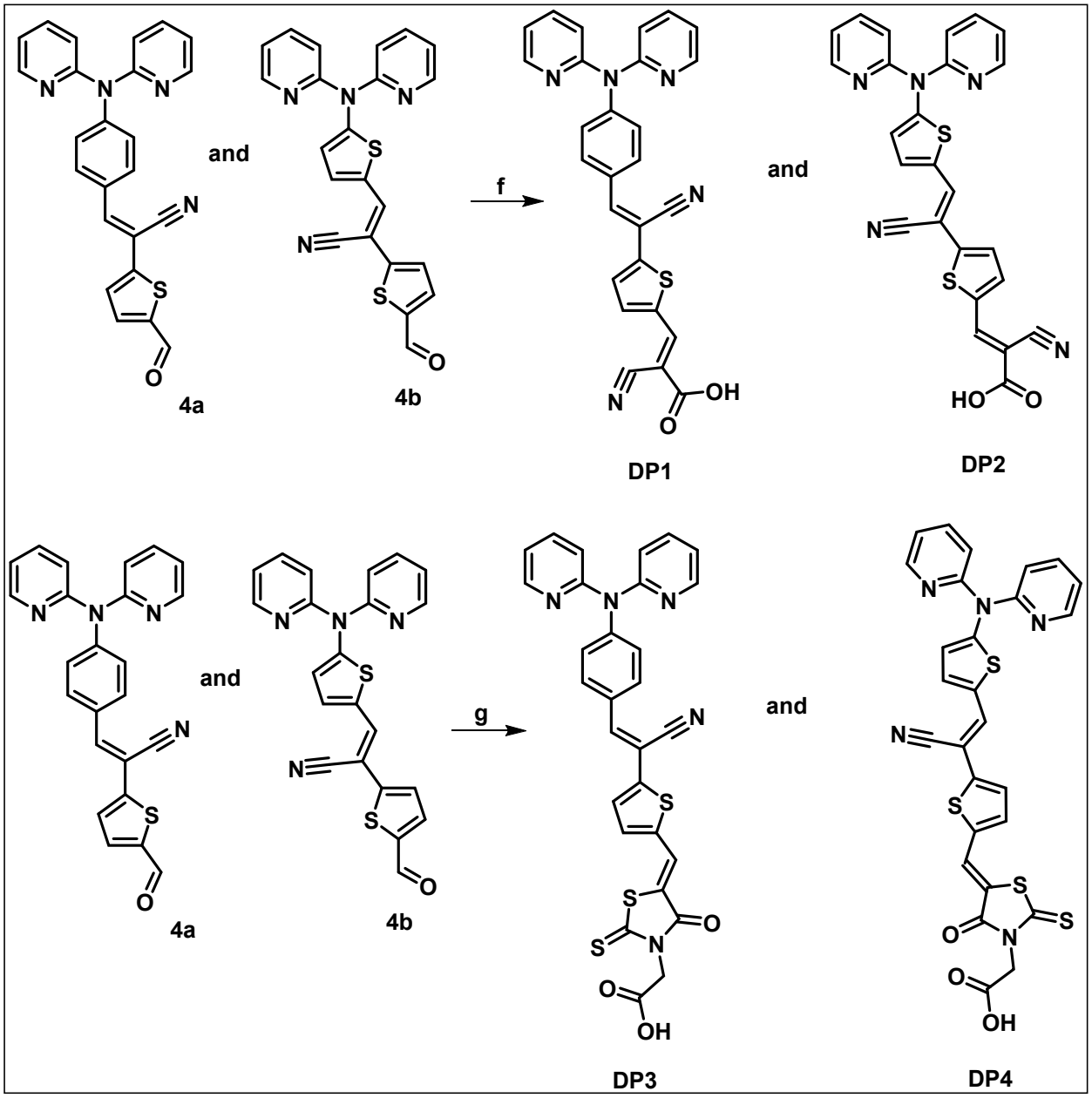


Scheme 3. Synthesis of DP sensitizers: (f) cyanoacetic acid, acetonitrile, ammonium acetate, reflux. (g) rhodanine-N-acetic acid, ammonium acetate, acetic acid, reflux.

**2-((Z)-5-((5-((E)-1-Cyano-2-(4-(di(pyridin-2-yl) amino) phenyl) vinyl) thiophen-2-yl) methylene)-4-oxo-2-thioxothiazolidin-3-yl) acetic acid (DP3)**

Ammonium acetate (0.0477 mmol) was added to a solution of compound 4a (0.0477 mmol) and rhodanine-3-acetic acid (0.0572 mmol) in acetic acid (6 ml). The reaction mixture was refluxed for 2.5 hrs. After completion of the reaction (monitored by TLC), the reaction mixture was cooled to room temperature and poured into water. The product filtered washed with water then purified by solvent treatment (wash with diethyl ether) to afford compound **DP3** as a red solid (81 % yield).

$^{1}$H NMR (500 MHz, DMSO) $\delta_{ppm}$ 8.31 (d, *J* = 4.5 Hz, 2H), 8.17 (s, 1H), 8.01 (s, 1H), 7.96 (d, *J* = 8.7 Hz, 2H), 7.82 (d, *J* = 4.1 Hz, 1H), 7.78 – 7.74 (m, 2H), 7.59 (d, *J* = 3.9 Hz, 1H), 7.18 – 7.12 (m, 4H), 7.04 (d, *J* = 8.2 Hz, 2H), 4.72 (s, 2H).

$^{13}$C NMR (125 MHz, DMSO) $\delta_{ppm}$ 192.14, 167.69, 166.41, 157.48, 149.04, 148.20, 147.29, 142.51, 138.85, 137.82, 131.26, 128.91, 128.32, 126.60, 125.53, 120.52, 120.18, 120.07, 118.46, 117.12, 102.42, 45.73

Elemental Analysis- Calculated: C, 59.88; H, 3.29; N, 12.04; O, 8.25; S,16.53.

View Article Online
DOI: 10.1039/C7NJ04620K
Journal Name ARTICLE

Found: C, 59.89; H, 3.28; N, 12.05.

**2-((Z)-5-((5-((E)-1-Cyano-2-(5-(di(pyridin-2-yl) amino) thiophen-2-yl) vinyl) thiophen-2-yl) methylene)-4-oxo-2-thioxothiazolidin-3-yl) acetic acid (DP4)**

This was prepared as described in the preparation of **DP3**. The residue was purified by solvent treatment (wash with diethyl ether) to afford compound **DP4** as a dark blue solid (84% yield).

$^{1}$H NMR (500 MHz, DMSO) $\delta_{ppm}$ 8.55 (dd, *J* = 4.9, 1.1 Hz, 2H), 8.11 (d, *J* = 3.1 Hz, 2H), 7.90 (td, *J* = 8.1, 1.9 Hz, 2H), 7.76 (d, *J* = 4.2 Hz, 1H), 7.62 (d, *J* = 4.5 Hz, 1H), 7.40 (d, *J* = 4.0 Hz, 1H), 7.36 – 7.32 (m, 2H), 7.00 (d, *J* = 8.2 Hz, 2H), 6.17 (d, *J* = 4.4 Hz, 1H), 4.70 (s, 2H).

$^{13}$C NMR (126 MHz, DMSO) $\delta_{ppm}$ 192.06, 167.73, 166.35, 154.19, 153.22, 149.14, 148.61, 140.00, 138.33, 137.27, 136.47, 135.63, 128.99, 126.81, 126.61, 121.59, 119.20, 118.01, 117.79, 115.73, 95.56, 45.67.

Elemental Analysis- Calculated: C, 55.18; H, 2.92; N, 11.92; O, 8.17; S, 21.82.

Found: C, 55.19; H, 2.91; N, 11.93.

**Fabrication and measurement of DSSC**

DSSC were fabricated as per our previously reported method [53] using sandwich type configuration of photoelectrode and counter electrode. FTO coated glass substrate was cleaned with the soap solution, water, and ethanol followed by 10 min sonication in every step. Using this cleaned substrate, photoelectrode was made from the commercial $TiO_2$ nanocrystalline semiconductor (P25, Sigma Aldrich). A thin film of the $TiO_2$ particles was deposited through screen printing from the $TiO_2$ paste containing ethyl cellulose and α-terpineol. The electrodes were calcined in a tubular furnace at 450 °C for 25 minutes and then soaked in the 10 mM dye solution. Dye soaking of the photoelectrode was carried out in a glove box filled with nitrogen under very low light level for 24 h. Counter electrodes were fabricated by spin coating of 50 mM $H_2PtCl_6$ solution in isopropanol onto pre-drilled FTO substrate followed by sintering at 450 ºC for 15 min. Dye coated photoelectrode and Pt counter electrode were sealed together using hot melt sealing tape upon application of heat. Electrolyte solution comprises of the 0.5 M 1-butyl-3-methylimidazolium iodide, 0.05 M $I_2$, 0.5 M TBP, 0.5M GSCN in 3-methoxy propionitrile, was inserted through the predrilled holes onto the counter electrode. Holes were sealed using epoxy adhesive and cover glass. DSSC were stored in dark at room temperature for 12 hours prior to measurements. The active area of the DSSC was set to 0.16 $cm^2$ and was maintained constant using the same screen for coating. The thickness of the $TiO_2$ nanocrystalline layer was 12 μm.

## Conclusions

Manipulation in novel metal-free organic sensitizers DP1, DP2, DP3, and DP4 having N-phenyl-N-(pyridin-2-yl) pyridine-2-amine (DPPA) and N-(pyridin-2-yl)-N-(thiophen-2-yl) pyridine-2-amine (DPTA) groups acting as electron donor. All the sensitizers have thiophene acetonitrile π- conjugation systems which are attached to cyanoacetic acid and rhodanine-3-acetic acid as anchoring groups. Their structural, electrochemical, optical properties were performed, and device fabrication studies were carried out to evaluate the manipulation effect. It is important to note that the absorption maximum values were red shifted in the order DP1 < DP3 < DP2 < DP4. The thiophene acetonitrile linker in all above sensitizers but DP4 had higher absorption maxima due to the presence of DPTA donor group and rhodamine-3-acetic acid. The sensitizer (DP2) comprising of DPTA donor group with thiophene acetonitrile as a π-spacer and cyanoacetic acid as an acceptor group shows good efficiency as compared with other sensitizers having same or different donors with same or different acceptor like rhodanine-3-acetic acid. The significant trend in molar extinction coefficient was observed in the order DP3 < DP4 < DP1 < DP2, the sensitizer DP2 had a higher value of molar extinction coefficient than the other sensitizers due to DPTA donor group and cyanoacetic acid anchoring group. It is concluded that, the DP2 is superior sensitizer for photovoltaic performance than the other DP sensitizers.

## Conflicts of interest

There are no conflicts to declare.

## Acknowledgements

One of the author, Dinesh Patil is thankful to UGC-SAP, India for Junior and Senior Research Fellowship. Authors thank to DST-CERI, New Delhi (DST/TM/CERI/C285(C) for the financial assistant. SSS and KKS are also thankful to UGC, New Delhi for funding under CPEPA program (Phase II).

## Notes and references

1 B. Pashaei, H. Shahroosvand, M. Graetzel and M. K. Nazeeruddin, *Chem. Rev.*, 2016, **116**, 9485–9564.
2 B. O'Regan and M. Grätzel, *Nature*, 1991, **353**, 737–740.
3 Z. L. Wang and W. Wu, *Angew. Chem. Int. Ed. Engl.*, 2012, **51**, 11700–21.
4 M. G. Tzel, *Acc. Chem. Res.*, , DOI:10.1021/ar900141y.
5 K. Ladomenou, V. Nikolaou, G. Charalambidis and a G. Coutsolelos, *Dalt. Trans.*, 2016, **45**, 1111–1126.
6 D. Wei, *Int. J. Mol. Sci.*, 2010, **11**, 1103–1113.
7 F.-T. Kong, S.-Y. Dai and K.-J. Wang, *Adv. Optoelectron.*, 2007, **2007**, 1–13.
8 M. Grätzel, *J. Photochem. Photobiol. C Photochem. Rev.*, 2003, **4**, 145–153.
9 A. Hagfeldt, G. Boschloo, L. Sun, L. Kloo and H. Pettersson, *Chem. Rev.*, 2010, **110**, 6595–6663.
10 C. Pavan Kumar, V. Anusha, K. Narayanaswamy, K. Bhanuprakash, A. Islam, L. Han, S. P. Singh and M. Chandrasekharam, *Inorganica Chim. Acta*, 2015, **435**, 46–

View Article Online
DOI: 10.1039/C7NJ04620K




52.
11 K. S. V Gupta, S. P. Singh, A. Islam, L. Han and C. M., *Electrochim. Acta*, 2015, **174**, 581–587.
12 A. Mishra, M. K. R. Fischer and P. Bäuerle, *Angew. Chem. Int. Ed. Engl.*, 2009, **48**, 2474–99.
13 Y. Cui, Y. Wu, X. Lu, X. Zhang, G. Zhou, F. B. Miapeh, W. Zhu and Z. S. Wang, *Chem. Mater.*, 2011, **23**, 4394–4401.
14 S. Yang, J. Liu, P. Zhou, K. Han and G. He, *Chem. Phys. Lett.*, 2011, **512**, 66–69.
15 J. Wu, G. Li, L. Zhang, G. Zhou and Z. Wang, *J. Mater. Chem. A*, 2016, **0**, 1–14.
16 Z. S. Wang, Y. Cui, Y. Dan-oh, C. Kasada, A. Shinpo and K. Hara, *J. Phys. Chem. C*, 2007, **111**, 7224–7230.
17 X. Zarate, F. Claveria-Cadiz, D. Arias-Olivares, A. Rodriguez-Serrano, N. Inostroza and E. Schott, *Phys. Chem. Chem. Phys.*, 2016, **18**, 24239–24251.
18 K. Hara, K. Sayama, H. Arakawa, Y. Ohga, A. Shinpo and S. Suga, *Chem. Commun.*, 2001, 569–570.
19 K. Sayama, S. Tsukagoshi, K. Hara, Y. Ohga, A. Shinpou, Y. Abe, S. Suga and H. Arakawa, *J. Phys. Chem. B*, 2002, **106**, 1363–1371.
20 A. Ehret, L. Stuhl and M. T. Spitler, *J. Phys. Chem. B*, 2001, **105**, 9960–9965.
21 D. D. Babu, S. R. Gachumale, S. Anandan and A. V. Adhikari, *Dye. Pigment.*, 2015, **112**, 183–191.
22 L. Wang, P. Shen, Z. Cao, X. Liu, Y. Huang, C. Liu, P. Chen, B. Zhao and S. Tan, *J. Power Sources*, 2014, **246**, 831–839.
23 S. S. M. Fernandes, M. C. R. Castro, I. Mesquita, L. Andrade, A. Mendes and M. M. M. Raposo, *Dye. Pigment.*, 2017, **136**, 46–53.
24 S. S. Soni, K. B. Fadadu, J. V. Vaghasiya, B. G. Solanki, K. K. Sonigara, A. Singh, D. Das and P. K. Iyer, *J. Mater. Chem. A*, 2015, **3**, 21664–21671.
25 Y. Hua, S. Chang, H. Wang, D. Huang, J. Zhao, T. Chen, W. Y. Wong, W. K. Wong and X. Zhu, *J. Power Sources*, 2013, **243**, 253–259.
26 G. Wu, F. Kong, J. Li, W. Chen, C. Zhang, Q. Chen, X. Zhang and S. Dai, *Synth. Met.*, 2013, **180**, 9–15.
27 H. Tan, C. Pan, G. Wang, Y. Wu, Y. Zhang, Y. Zou, G. Yu and M. Zhang, *Org. Electron. physics, Mater. Appl.*, 2013, **14**, 2795–2801.
28 Z. S. Wang, Y. Cui, K. Hara, Y. Dan-Oh, C. Kasada and A. Shinpo, *Adv. Mater.*, 2007, **19**, 1138–1141.
29 X. Chen, C. Jia, Z. Wan and X. Yao, *Dye. Pigment.*, 2014, **104**, 48–56.
30 C. Teng, X. Yang, C. Yuan, C. Li, R. Chen, H. Tian, S. Li, A. Hagfeldt and L. Sun, 2009, 11–14.
31 M. Liang and J. Chen, *Arylamine organic dyes for dye-sensitized solar cells*, 2013, vol. 42.
32 Z. Ning, Q. Zhang, W. Wu, H. Pei, B. Liu and H. Tian, *J. Org. Chem.*, 2008, **73**, 3791–3797.
33 T. Kaewpuang, N. Prachumrak, S. Namuangruk, S. Jungsuttiwong, T. Sudyoadsuk, P. Pattanasattayavong and V. Promarak, *European J. Org. Chem.*, 2016, **2016**, 2528–2538.
34 C. Chitpakdee, S. Jungsuttiwong, T. Sudyoadsuk, V. Promarak, N. Kungwan and S. Namuangruk, *Spectrochim. Acta Part A Mol. Biomol. Spectrosc.*, 2017, **174**, 7–16.
35 S. Huang, Y. Hsu, Y. Yen, H. H. Chou, T. Lin, C. Chang, C. Hsu, C. Tsai, D. Yin and J. T. Lin, *J. Phys. Chem. C*, 2008, 19739–19747.
36 W. Wu, J. Yang, J. Hua, J. Tang, L. Zhang, Y. Long and H. Tian, *J. Mater. Chem.*, 2010, **20**, 1772.
37 Z. Wan, C. Jia, J. Zhang, Y. Duan, Y. Lin and Y. Shi, *J. Power Sources*, 2012, **199**, 426–431.
38 O. Treutler and R. Ahlrichs, *J. Chem. Phys.*, 1995, **102**, 346–354.
39 A. D. Becke, *J. Chem. Phys.*, 1993, **98**, 1372–1377.
40 C. Lee, W. Yang and R. G. Parr, *Phys. Rev. B*, 1988, **37**, 785–789.
41 M. E. Casida, C. Jamorski, K. C. Casida and D. R. Salahub, *J. Chem. Phys.*, 1998, **108**, 4439–4449.
42 M. Cossi, V. Barone, R. Cammi and J. Tomasi, *Chem. Phys. Lett.*, 1996, **255**, 327–335.
43 J. Tomasi, B. Mennucci and R. Cammi, *Chem. Rev.*, 2005, **105**, 2999–3094.
44 G. E. M. J. F. G. W. T. H. B. Schlegel, G. A. S. M. A. R. J. R. C. G. S. V. B. B. Mennucci, J. P. H. N. M. C. X. L. H. P. H. A. F. Izmaylov, J. B. G. Z. J. L. S. M. H. M. E. K. T. R. Fukuda, J. A. H. M. I. T. N. Y. H. O. K. H. N. T. Vreven, K. N. M. J. J. E. P. F. O. M. B. J. J. H. E. Brothers, J. K. V. N. S. R. K. J. N. K. R. A. Rendell, J. E. C. B. S. S. I. J. T. M. C. N. R. J. M. M. M. Klene, R. E. S. K. J. B. C. V. B. C. A. J. J. R. Gomperts, K. O. Y. A. J. A. R. C. C. P. J. W. O. R. L. Martin, S. M. V. G. Z. G. A. V. P. S. J. J. Dannenberg, and D. D. A. D. D. O. F. J. B. F. J. V. O. J. Cioslowski and W. C. J. F. G. Inc., .
45 C. Adamo and D. Jacquemin, *Chem. Soc. Rev.*, 2013, **42**, 845–856.
46 Y. Wu and W. Zhu, *Chem. Soc. Rev.*, 2013, **42**, 2039–2058.
47 E. Ronca, G. Marotta, M. Pastore and F. De Angelis, *J. Phys. Chem. C*, 2014, **118**, 16927–16940.
48 J. Bisquert, *J. Phys. Chem. B*, 2002, **106**, 325–333.
49 J. V. Vaghasiya, K. K. Sonigara, K. B. Fadadu and S. S. Soni, *Perspect. Sci.*, 2016, **8**, 2–5.
50 Y. Wu, X. Zhang, W. Li, Z. S. Wang, H. Tian and W. Zhu, *Adv. Energy Mater.*, 2012, **2**, 149–156.
51 P. J. Cameron, L. M. Peter and S. Hore, *J. Phys. Chem. B*, 2005, **109**, 930–936.
52 J. N. Soderberg, A. C. Co, A. H. C. Sirk and V. I. Birss, *J. Phys. Chem. B*, 2006, **110**, 10401–10410.
53 R. L. Vekariya, K. K. Sonigara, K. B. Fadadu, J. V. Vaghasiya and S. S. Soni, *ACS Omega*, 2016, **1**, 14–18.

View Article Online
DOI: 10.1039/C7NJ04620K



## Table of Contents:

Insertion of heteroatom in triarylamine donor along with variation in anchoring groups finely manipulate the photophysical and photovoltaic structure to property behaviour of D-A'-π-A sensitizers in DSSCs for better efficiency achievement.